RAPID DETECTION AND LOCALIZATION OF SPECIAL NUCLEAR MATERIALS

Jana Petrović, Alf Göök, Débora M. Trombetta, and Bo Cederwall

Department of Physics, KTH Royal Institute of Technology, SE-10691 Stockholm, Sweden

ABSTRACT

We report on the development of a novel approach to sensitive detection and imaging of special nuclear materials (SNM) within the context of an organic scintillator-based radiation portal monitor (RPM) prototype system. The system uses fast time- and energy correlations between detected neutrons and gamma rays as an additional detection modality for achieving enhanced sensitivity for SNM with low false alarm rates. Rapid and precise localization of small amounts of SNM within the field of view is made possible using the newly developed neutron-gamma emission tomography (NGET) technique. This novel imaging modality addresses global security threats from terrorism and the proliferation of nuclear weapons. It is versatile and can readily be adapted to different detection geometries in different applications for nuclear security, public safety, nuclear accident scenarios and radiological surveying in various contexts.

1. INTRODUCTION

The detection of special nuclear materials (SNM) in Radiation Portal Monitors (RPMs) is one of the critical links in the nuclear security chain. A characteristic signature of such materials is the emission of neutrons from spontaneous fission or (α,n) reactions. RPMs designed to be sensitive to the presence of SNM detect neutrons and commonly use detectors based on ^{3}He proportional counters, which are thermal neutron detectors typically surrounded by moderating materials. Due to the global shortage of ^{3}He there is a large interest in developing ^{3}He free systems [1]. In addition to detection schemes replacing ^{3}He with other high-neutron-absorption cross section materials like boron and lithium there is also an increasing focus on direct fast-neutron detection based on organic scintillators, high-pressure ^{4}He systems [2] etc. Organic-scintillator-based detectors have been found to compare favorably in terms of absolute detection efficiency with the "gold standard" ^{3}He-based systems [3]. However, there are important issues related to "nuisance" alarms and difficulties in detecting small quantities of SNM, in particular in shielded environments, reported in the literature. A novel approach [4] that addresses these issues utilizes the high multiplicity and short time-of-flight of gamma rays and their short time correlations with fast neutrons as a unique signature of materials that undergo spontaneous or induced fission, such as SNM. By making use of gamma-fast neutron coincidence counting as an additional detection modality in parallel with standard single gamma and neutron counting the RPM false alarm rate (FAR) can be increased significantly, while neutron-neutron coincidence counting often is prohibitively inefficient [5]. Efficient localisation of SNM within the field of view is also made possible using a novel imaging modality, neutron-gamma emission tomography (NGET) [6]. Moreover, the use of coincidences adds to the system an enhanced capability of quantifying and characterizing the material of interest, expanding the applications from prevention of nuclear material trafficking to accountability and control.

2. HARDWARE DESIGN AND DATA PROCESSING

The KTH prototype RPM is a modular organic scintillator-based system with an easily modified geometry that can be adapted to different applications. We here report on results obtained using a configuration that is well suited for different package/conveyor as well as pedestrian RPM applications. Results from sensitivity measurements for a different, more compact geometry were reported in Ref. 5. Organic scintillators have high gamma-ray and neutron efficiencies as well as excellent neutron/gamma pulse shape discrimination and timing properties. The general system geometry is adapted to the ANSI N42.35-2016 industry standard [7] and is modular and therefore easily scalable. In addition to high gamma-ray and neutron detection efficiencies the system additionally makes use of the fast-timing properties of the organic scintillator to enhance the detection sensitivity and identification of special nuclear materials (SNM) [4].

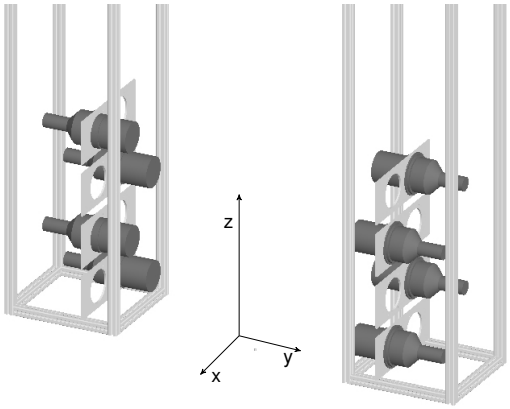

FIG. 1. Schematic drawing of the RPM prototype system showing the two detection assemblies and the partially occupied mechanical support structure. The horizontal distance between the front faces of the detection assemblies is 1.0m, in accordance with the industry standard ANSI N42.35-2016.

The RPM prototype system was evaluated in a geometry consisting of two pillars with one detection assembly in each pillar. A total of eight 127 mm diameter by 127 mm length cylindrical cells were arranged in two detector arrays, each forming a zig-zag pattern (Fig. 1). Each detector cell, containing approximately 1.6 l of EJ-309 scintillator [8], was optically coupled to a Hamamatsu R1250 photomultiplier tube (PMT) [9]. The PMT anode pulses were read out by an 8-channel digitizer board featuring 14 bit resolution and 500 MHz sampling rate. The digitizer board features firmware programmable pulse shape discrimination (PSD) capabilities for distinguishing between neutron and gamma-ray interactions in the scintillators based on field programmable gate arrays (FPGA). The support structure is designed to accommodate up to 20 horizontally oriented detector cells in each pillar and additionally ten detector cells at the top of the structure making up a total of 50 detector cells. An increase in the solid-angle coverage and detection efficiency is recommended for the most challenging applications. Other, completely different, detection geometries, e.g. based on a rectangular tiling, are also easily accommodated within the same support structure. For further details concerning the detection assembly and readout electronics see Ref. 5. The digitized signals ("traces") from the RPM detector modules are processed in real time within the digitizer's FPGAs to extract charge integrals, pulse shape information and timing information. The PSD algorithm for distinguishing gamma-ray interactions from neutron interactions is based on the charge comparison method as illustrated in Fig. 2 whereas sharp time stamp extraction is performed using a digital constant fraction discrimination algorithm. Energy information for

each trace is extracted using a moving window de-convolution algorithm. The resulting processed data stream contains information on single-neutron and gamma count rates as well as fast coincidence rates for gamma-neutron, neutron-neutron, and gamma-gamma events with adjustable coincidence time windows and thresholds. Typical coincidence time windows are 0-100 ns for gamma-gamma and neutron-neutron events and 10-100 ns for gamma-neutron events.

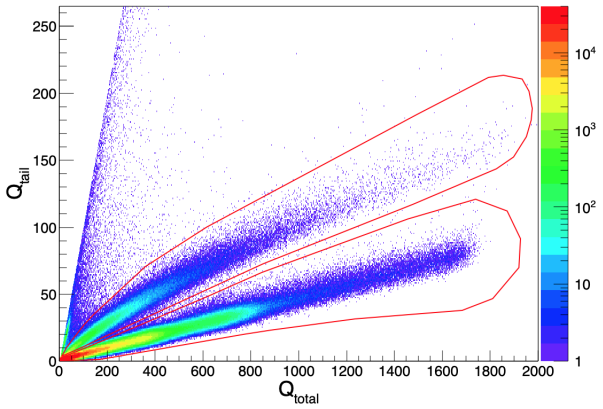

FIG. 2. Total (sum of all detectors) pulse-shape discrimination (PSD) plot showing the distribution of tail integrals (taken over the last 73% of the signals) vs the full integrals of the PMT signals. The vertical color scale is indicated on the right. Neutrons and gamma rays were selected by choosing events within the regions indicated by the red line (upper and lower region, respectively. The signals saturate at around 6.5 MeV_{ee}.

3. SENSITIVITY MEASUREMENTS

3.1 Background evaluation

The ANSI standard background conditions for performing radiological tests of RPMs are 5-10μR/h for gamma radiation and less or equal to 200 neutrons $s^{-1}m^{-2}$. Standard neutron-sensitive RPMs containing ^{3}He counters or similar thermal neutron detectors are sensitive to the full cosmic ray neutron spectrum including the down-scattered neutrons, without preserving incident neutron energy information. On the other hand, organic-scintillator-based detection systems, are only sensitive to fast neutrons. Therefore, the neutron background levels in such systems are significantly reduced compared with the dominant thermal neutron background from down-scattering of cosmic-ray-induced neutrons. In organic-scintillator detectors employed in PSD mode the main contribution to the neutron background count rate is due to particle misidentification where background gamma-rays are misinterpreted as neutrons as an effect of electronic noise or pile-up. It is proportional to the average singles gamma rate in the scintillators with a factor typically around one to a few per mille [10] depending on the PSD cuts applied. In a study of the fast-neutron background in different environmental conditions using similar liquid organic-scintillator detectors and a similar neutron-gamma discrimination technique as in the present work, a mean neutron count rate for neutron energies deposited in the detectors above 500 keV of around 2.2 s^{-1} was reported at near sea-level elevation and normal atmospheric pressure in a total active detection volume of approximately 25 l [11]. This scales well with the detector volume for the background rates measured with the RPM prototype system inside the KTH Nuclear Physics detector laboratory (Table 1) and is somewhat lower than the previous preliminary measurement [5] following fine tuning of

detection thresholds. The radiation background dose rate in this environment is around 0.2μSv/h. It is noteworthy that the system was unshielded in the presently reported configuration and therefore subject to a much higher gamma-ray background count rate than would be the case using 10 mm or more of lead shielding installed on the outer sides of each pillar, which is typical for standard commercial systems.

Table 1. Background count rates measured in the KTH detector laboratory. No detector shielding was applied. The energy thresholds for gamma rays and neutrons were 20 keV and 500 keV, respectively.

	Counts/s
Single neutrons	1.000 ± 0.002
Single gamma rays	5189.0 ± 0.2
Gamma-neutron coinc.	0.0030 ± 0.0002
Gamma-gamma coinc.	63.00 ± 0.02
Neutron-neutron coinc.	0.0021 ± 0.0001

3.2 False alarm rate tests

A “false alarm” is defined as the declaration of an alarm due a measurement of counts during the relevant measurement period, in this case one second, in any of the measured parameters (neutrons, gamma-rays, gamma-neutron coincidences, neutron-neutron coincidences, etc) when no radiation source other than room background is present. The ANSI N42.35-2016 RPM evaluation standard document [7] does not specifically take into account systems which are able to measure fast coincidence events, as in the present case, even though the same basic principles apply. The document describes a false alarm test method and sets as an acceptable result if no more than 1 false alarm occurs in 1000 occupancies for systems with occupancy sensor, or no more than 1 alarm in 2 hours of observation in systems without occupancy sensor. The KTH RPM prototype system can be operated with or without occupancy sensor. The 4σ alarm thresholds relevant for an interrogation time of 1 s with background conditions as measured in the KTH detector lab are given in Table 2. The probability to observe one gamma-neutron coincidence count in a one second interrogation period due to room background was measured to be 0.003. In only one case was two gamma-neutron coincidence events observed during 221 000 consecutive measurements corresponding to a FAR of the order of 4×10^{-6}.

Table 2. Alarm trigger thresholds (approximately 4σ above mean background count rates)

	counts/s
Single neutrons	5
Single gamma rays	5477
Gamma-neutron coinc.	1
Neutron-neutron coinc.	1

3.3 Source tests

The response of the RPM system was measured using radioactive lab sources of ^{133}Ba, ^{137}Cs, and ^{252}Cf. The results were used to calculate the sigma multiplier factor [12] in order to assess the performance of the KTH RPM prototype in the present 8-module "zig-zag" configuration. The sigma multiplier satisfies the condition that the sum of the background counts, C and the product of its standard deviation sigma, σ_B and the sigma multiplier factor, N, equals the mean counts measured during a given interrogation time (source + background): $\langle C_B \rangle + N \times \sigma_B = \langle C_S + C_B \rangle$. Here, we evaluate the sigma multiplier factor for detection of single neutrons, gamma-neutron coincidences and neutron-neutron coincidences for a measurement time of one second while the source is moving through the RPM at 1.2 m/s (i.e covering the distance from -0.6 m to +0.6 m), where the origin is at the centre of the detection system, see Tables 3 and 4. Considering detection thresholds of 4σ above the mean background (see Table 2) we also give the probabilities of a false negative result, p_N (i.e that the passage of the source was not detected) for the different detection modes in Tables 3 and 4. Before the measurements the individual detectors were gain matched using standard radioactive calibration sources; the internal conversion K X-ray photopeak and Compton edge for ^{137}Cs (32 KeV and 478 keV, respectively) and the 59.5 keV photopeak of ^{241}Am.

3.3.1 ^{252}Cf

The measured response to the passage of a ^{252}Cf source with a neutron emission rate of approximately 5400 n/s is summarized in Table 3. This source has an activity of around 27% of the ANSI N42.35-2016 standard ^{252}Cf source [7]. The ^{252}Cf material is embedded in a ceramic cylinder with dimensions 4.6 mm (diam.) by 6 mm and encapsulated in a double-welded stainless-steel cylinder with outer dimensions 7.8 mm (diam.), 10.0 mm (ANSI classification code C66544) [13]. While the highest sigma multiplier factor and a correspondingly low FAR are achieved for the gamma-neutron coincidence mode the highest statistics and lowest false-negative probability is achieved for single-neutron counting for such a relatively weak source. The best overall performance is hence obtained by combining the information obtained from the single-neutron and fast-neutron-gamma coincidence rates.

Table 3. Alarm tests - ^{252}Cf .

SOURCE NEUTRON EMISSION RATE	SINGLE NEUTRONS N / p_N	GAMMA-NEUTRON COINCIDENCES N / p_N	NEUTRON-NEUTRON COINCIDENCES N / p_N
5400 n/s	$30 / 6 \cdot 10^{-9}$	38 / 0.12	4 / 0.84

3.3.2 ^{137}Cs and ^{133}Ba

The measured response to the passage of ^{137}Cs (activity 184 kBq) and ^{133}Ba (activity 44 kBq) gamma-ray sources are summarized in Table 4. The sources are significantly weaker than required in the ANSI N42.35-2016 standard, 9.6% and 32% of the ANSI standard activities for ^{133}Ba and ^{137}Cs, respectively. The gamma-ray "surrogate" for weapons grade plutonium (WGPu) is ^{133}Ba with an activity of 120 kBq , corresponding to 1 g of WGPu. The results show

excellent detection capabilities for these relatively weak sources. In the case of the ^{133}Ba source the activity only produces an increase of approximately 14% in the count rate over the normal background rate.

Table 4. Alarm tests - ^{137}Cs and ^{133}Ba.

SOURCE	ACTIVITY	SIGMA MULTIPLIER (N)	PROBABILITY OF FALSE NEG. (p_N)
^{133}Ba	44 kBq	8	$3 \cdot 10^{-4}$
^{137}Cs	184 kBq	28	$<10^{-12}$

4. 3D SOURCE LOCALIZATION

Due to its granularity and fast-timing properties the KTH RPM prototype system has excellent 3D-imaging capabilities for SNM imaging based on the principle of neutron-gamma emission tomography (NGET) [6]. In the present work, examples of the imaging capabilities for the new geometrical zig-zag detector configuration are given. Additionally, effects of plastic and lead shielding on the image resolution have been investigated. The plastic shielding consisted of an ultra-high molecular weight polyethylene (UHMWPE/PE1000) cylinder of 44 mm outer radius, 4.0 mm inner radius, and 83 mm height. The lead shielding consisted of a lead cylinder with 31 mm outer radius, 15 mm inner radius, and 105 mm height. The encapsulated Cf-252 source was placed in the geometrical center of the shielding in both cases. Fig. 3 shows results of source localization using Bayesian inference [6] for the Cf-252 source described in section 3.3.1 without additional shielding as well as for the PE1000 and lead shielding. For each of the three positions (with coordinates as defined in Fig. 1): (x,y,z) = (0,-30,22) cm, (0,0,52) cm, and (0,30,82) cm, the images show typical probability density functions following Bayesian updating for data acquired during a 10 s measurement time. In Fig. 4 the 3D-image of the source in a different position, (x,y,z) = (20,-30,52) cm, is illustrated by projecting the image in the xy, xz, and yz-planes. While there are signs of some loss of image resolution with the introduction of plastic and lead shielding the effects are relatively modest for the presently investigated cases, the spatial uncertainty of the localization remaining in the range 1 to a few cm (sigma).

5. DISCUSSION

Minimizing the risks to public safety and international security from illegal trafficking of nuclear or other radioactive materials requires versatile detection systems that can efficiently detect radiological threats in real time. The possibility to rapidly and precisely locate SNM, at, e.g., border controls, postal mail centers or transport hubs would provide an important tool for counter-terrorism measures and non-proliferation efforts. 3D-imaging of SNM also has several other important potential applications, such as for nuclear emergency response, spent fuel verification in nuclear safeguards and environmental surveying. In the recent work of Steinberger et al. [14] a state-of-the-art compact 2D radiation imaging system for SNM was presented based on the principle of neutron scatter imaging with organic scintillation detectors. The NGET imaging technique used in the present work enables localization of SNM in 3D with higher accuracy and orders of magnitude higher efficiency [6] than other neutron imaging

techniques. An important reason for the higher performance obtained here compared with, e.g., neutron scatter imaging is the use of the fundamental properties of gamma-fast neutron correlations from nuclear fission, in particular the emission of multiple, prompt gamma-rays with a high average multiplicity.

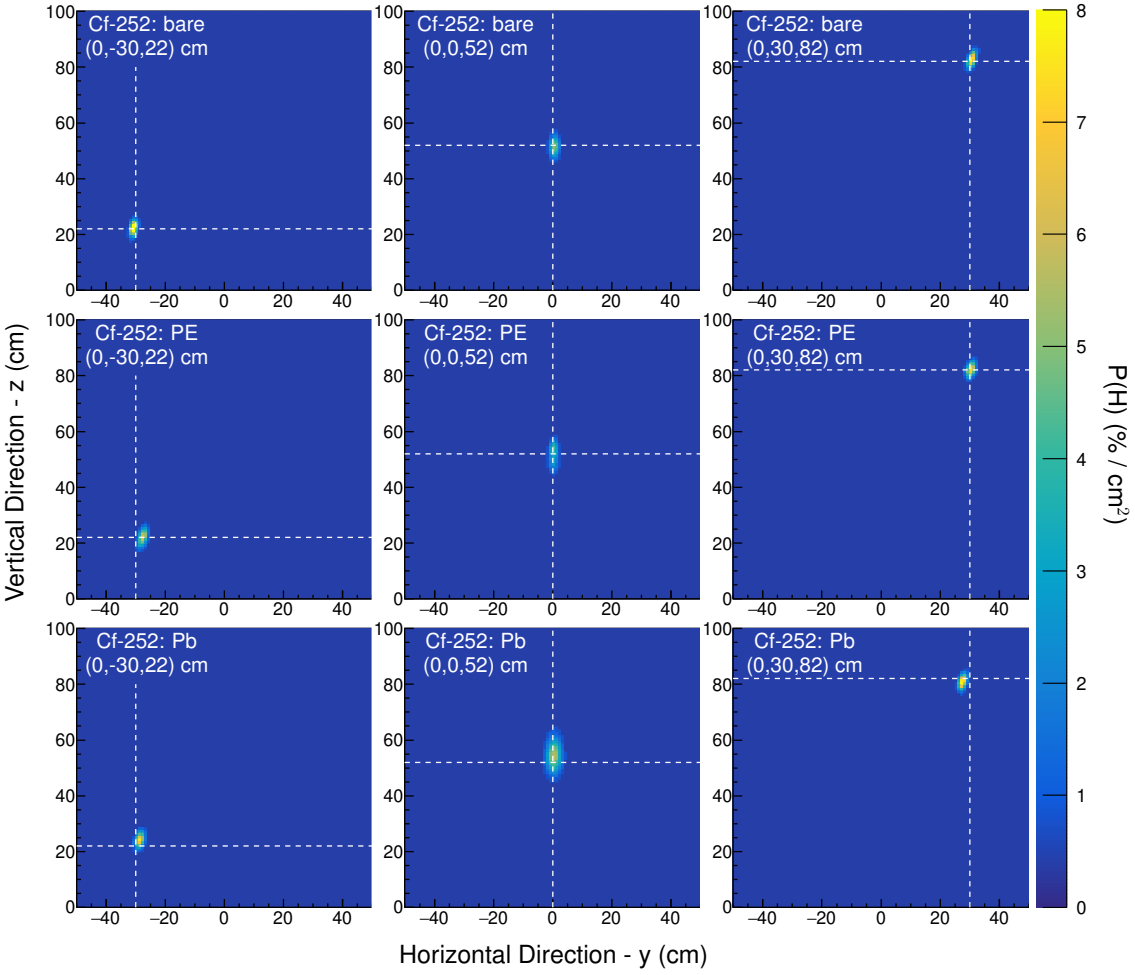

FIG. 3. Demonstration of source localization using the Bayesian inference algorithm. The panels in each column corresponds to a 10 s measurement of the Cf-252 source described in section 3 at a different source position. The top row shows results for the bare source, the middle row shows results for measurements of the same source encapsulated in the PE1000 shielding while the bottom row shows results for measurements with the Pb shielding (see text for details). The source positions are indicated by a dashed white cross-hair. The color scale indicates the probability of finding the source per cm² pixel as calculated by the source localization algorithm.

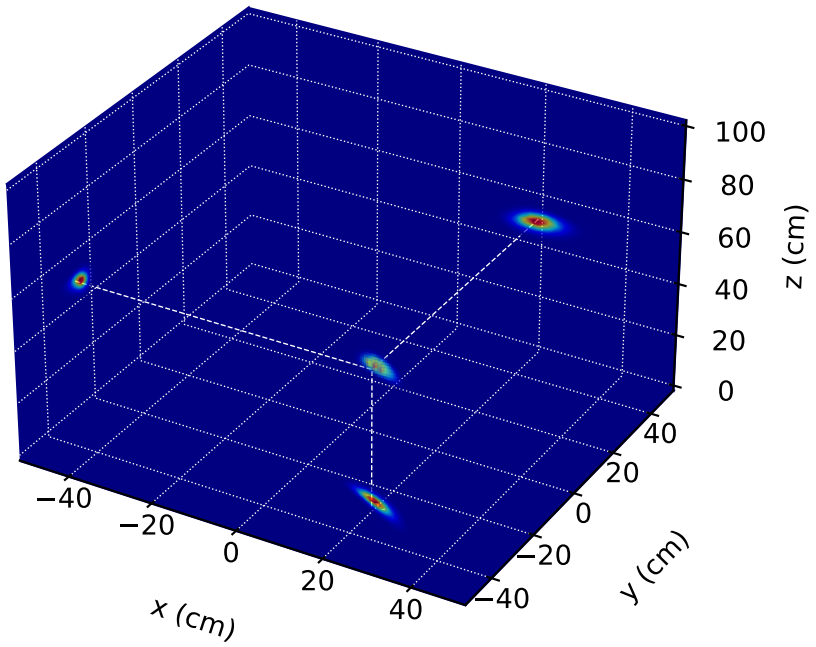

FIG. 4. 3D representation of the Cf-252 source localization. The source was measured during 10 s and shielded by 4 cm HDPE and placed at a position (x,y,z) = (20,-30,52) cm. See text for details.

6. CONCLUSIONS AND OUTLOOK

A pedestrian/package/luggage RPM system based on organic liquid scintillation detectors has been designed and tested in a limited-scaled prototype version at KTH Royal Institute of Technology. The system has been shown to be able to consistently alarm for standard gamma-ray and neutron sources under conditions outlined in the ANSI N42.35-2016 standard document and beyond. For sources undergoing spontaneous fission the ability to apply the novel gamma-neutron coincidence mode in addition to standard single-neutron counting provides the lowest false alarm rate and low false negative rates in conjunction with new imaging capabilities [6]. The 3D-imaging performance has been shown to remain in the presence of a few cm of plastic and lead shielding with only moderate loss of spatial resolution. The demonstrated ability to rapidly localize small amounts of nuclear materials with high accuracy opens the possibility for a paradigm shift in national security applications, nuclear safeguards, environmental surveying, and for nuclear emergency responders. Each application has its own challenges that will require special attention. For RPM systems designed for larger objects like vehicles and shipment containers the potential presence of significant amounts of heavy shielding materials is of particular interest and deserves further studies.

7. ACKNOWLEDGEMENTS

This work was supported by the Swedish Radiation Safety Authority under contract Nos. SSM2016-3954, SSM2018-4972, and SSM2018-4393, the Swedish Innovation Agency (Vinnova) under contract No. VFT-1 245, and Carl Tryggers Stiftelse för Vetenskaplig Forskning under contract No. CTS 14:89.

REFERENCES

[1] Pickrell, M.M., et al., The IAEA workshop on requirements and potential technologies for replacement of 3He detectors in IAEA safeguards applications, J. Nucl. Mater. Manage. 41 (2) (2013).
[2] Lewis, J.M.; R. P. Kelley; D. Murer; K. A. Jordan, "Fission signal detection using helium-4 gas fast neutron scintillation detectors". Appl. Phys. Lett. 105 (2014) 014102.
[3] Pozzi, S.A. et al., Comparative neutron detection efficiency in ^{3}He proportional counters and liquid scintillators, Nucl. Instrum. Meth. Phys. Res. A 929 , (2019) 107.
[4] Trombetta, D.M.; Klintefjord, M.; Axell, K.; Cederwall, B., Fast neutron and γ-ray coincidence detection for nuclear security and safeguards applications, Nuclear Instrumentations and methods in physics research, A. 927 (2019) 119-124.
[5] D. Trombetta, C. Sundaram, K. Axell, and B. Cederwall, 'Sensitive detection of special nuclear materials for RPM applications based on gamma-fast neutron coincidences', Proc. International Conference on Nuclear Security, 8710 (2020).
[6] Jana Petrović, Alf Göök, and Bo Cederwall, 'Rapid imaging of special nuclear materials for nuclear nonproliferation and terrorism prevention', Science Advances, Vol. 7, no. 21, eabg3032 (2021)
[7] ANSI N42.35-2016, American National Standard for Evaluation and Performance of Radiation Detection Portal Monitors for Use in Homeland Security, DOI: 10.1109/IEEESTD.2016.7551097.
[8] Eljen Technology, Neutron/gamma PSD liquid Scintillator EJ-301, EJ-309, <https://eljentechnology.com/products/liquid-scintillators/ej-301-ej-309 > (accessed 20 November 2019).
[9] https://www.hamamatsu.com/eu/en/product/type/R1250/ (accessed 28 November 2019).
[10] Cederkäll, J., et al. Nucl. Inst. Meth. Phys Res. A 385 (1997) 166.
[11] Davis, J.R., Brubaker, E., Vetter, K. Fast neutron background characterization with the Radiological Multisensor Analysis Platform (RadMAP), Nucl. Instrum. Meth. Phys. Res. A 858, (2017) 106.
[12] IAEA, Nuclear Security Series No.1, Technical and Functional Specifications for Border Monitoring Equipment (2016).
[13] Sealed Radiation Sources, Product Information – Eckert & Ziegler Nuclitec GmbH, Rev. 07 /2009.
[14] W. M. Steinberger, et al., Scientific Reports 10, 1855 (2020).